Effects of die land length and geometry on curvature and effective strain of profiles produced by a novel sideways extrusion process

Zhou, Wenbin; Yu, Junquan; Lin, Jianguo; Dean, Trevor A.

DOI:
10.1016/j.jmatprotec.2020.116682

Document Version
Peer reviewed version

Citation for published version (Harvard):
Zhou, W, Yu, J, Lin, J & Dean, TA 2020, 'Effects of die land length and geometry on curvature and effective strain of profiles produced by a novel sideways extrusion process', *Journal of Materials Processing Technology*, vol. 282, 116682. https://doi.org/10.1016/j.jmatprotec.2020.116682

Journal Pre-proof

Effects of die land length and geometry on curvature and effective strain of profiles produced by a novel sideways extrusion process

Wenbin Zhou (Conceptualization) (Methodology) (Validation) (Investigation) (Formal analysis) (Data curation) (Visualization) (Writing - original draft), Junquan Yu (Conceptualization) (Methodology)<ce:contributor-role>Writing - reviewing and editing), Jianguo Lin (Conceptualization) (Methodology)<ce:contributor-role>Writing - reviewing and editing) (Supervision), Trevor A. Dean (Conceptualization)<ce:contributor-role>Writing - reviewing and editing)

PII: S0924-0136(20)30096-0

DOI: https://doi.org/10.1016/j.jmatprotec.2020.116682

Reference: PROTEC 116682

To appear in: *Journal of Materials Processing Tech.*

Received Date: 12 December 2019

Revised Date: 3 March 2020

Accepted Date: 9 March 2020

Please cite this article as: Zhou W, Yu J, Lin J, Dean TA, Effects of die land length and geometry on curvature and effective strain of profiles produced by a novel sideways extrusion process, *Journal of Materials Processing Tech.* (2020), doi: https://doi.org/10.1016/j.jmatprotec.2020.116682

Effects of die land length and geometry on curvature and effective strain of profiles produced by a novel sideways extrusion process

Wenbin Zhou[a], Junquan Yu[a,*] , Jianguo Lin[a,], Trevor A. Dean[b]

[a]*Department of Mechanical Engineering, Imperial College London, London SW7 2AZ, UK*

[b]*Department of Mechanical Engineering, University of Birmingham, Birmingham B15 2TT, UK*

[*] Corresponding author. Tel.: +44 0 770 844 8885;

Email address: junquan.yu@imperial.ac.uk (Junquan Yu).

Abstract

In the present investigation, effects of length and geometry of die land/bearing on curved profiles/sections produced by a novel process, differential velocity sideways extrusion (DVSE), were studied through physical experiments using plasticine as a model material and finite element modelling. Profile curvature decreases as die land length increases due to its negative influence on exit velocity gradient, and a straight profile is extruded when the ratio of die land length to die orifice diameter exceeds a critical value l_0 which increases as extrusion ratio λ increases and extrusion velocity ratio v_2/v_1 decreases. Generally, effective strain level of the extrudate slightly increases as the die land length increases. Larger die land length increases the frictional areas between extrudate surface layers and die land (and mandrel for tube extrusion), generating zone of shear along the profile edge and thus increases surface layer effective strain. As a result, the strain homogeneity over the cross-section or wall thickness (for tube extrusion) is decreased. Compared with a sharp die land/container transition corner, a chamfered or radiused die land transition corner leads to an increased curvature due to the decreased effective land length, while it decreases overall effective strain level in the cross-section and strain homogeneity as a result of lower effective strain rate across the deforming region. A sharp die land transition corner is recommended for achieving a relatively large and homogenous effective strain in the cross-section.

Keywords: Differential velocity sideways extrusion (DVSE); Curved profiles/sections; Die land; Bearing length; Curvature; Strain inhomogeneity

1. Introduction

Extruded profiles/sections are widely used as basic elements to construct structural components as a result of their high strength/stiffness relative to weight. Lightweight structure design strategies using profiles are effective ways to contribute to less fuel/energy consumption and CO_2 emissions. In the industries of aerospace and automobile, curved profiles are extensively utilised in structures of vehicles on account of their ease for incorporation into aerodynamic forms. As pointed out by Tekkaya and Chatti (2014), since little machining and welding/joining effort is needed for curved profiles to meet structural requirements, increased manufacturing efficiency and improved aerodynamic properties for vehicle bodies can be achieved. Curved profiles having various cross-sections are also used in architecture as constructional elements to improve aesthetics and expand the feasible range of structural designs, as reported by Cruz (2013).

Currently, most of curved profiles are usually fabricated by bending a straight extruded profile, which not only leads to long manufacturing time (including extrusion and bending) and high production cost, but also cannot avoid some bending defects, such as wrinkling and crack. Vollertsen et al. (1999) have given a comprehensive overview of the various available curved profile forming techniques being developed and discussed their strengths and weaknesses, emphasising roll bending, rotary draw bending, stretch bending, and press bending. Yang et al. (2012) later made a detailed review specifically on tube (profiles with hollow cross sections) bending forming technologies. Generally, due to the bending force necessary to curve straight extrusions, three major kinds of bending defects, including cross-section distortion, wrinking, and springback, arise usually during bending process. To alleviate these, additional stress or torque with bending have been proposed. Chatti et al. (2007) proposed a modification of the roll bending process by superposing conventional three-roll bending with a movable bending tool. A local pre-plasticisation is generated by the initial three-roll bending in the forming zone of the workpiece, making further bending easier, thus subsequent bending force and springback are reduced. Hermes et al. (2015) proposed a torque superposed bending technique, in which distortion (twisting) of asymmetrical sections was compensated by superposition of torque with bending moment. To reduce forming procedures and improve efficiency, some extrusion-bending integrated processes have been proposed. Shiraishi et al. (2003) proposed using an inclined die orifice to extrude curved bars and tubes from conventional billets. Experiments were conducted where plasticine was utilised as workpiece and it was concluded that profile curvature could be altered

by varying the inclined angle of die orifice, an increase of which leads to increased curvature. Müller et al. (2006) used an external guiding tool during the conventional extrusion process to manufacture curved profiles, the profile curvature depends on the geometrical position of the external guide which is controlled by a linear axes system and moves synchronously with the speed of the extruded profile. Despite the quality improvement achieved by the current curved profile forming processes, they lack versatility and to enable profile curvature to be changeable along the length of a product, expensive complex tooling is necessary. In addition the mechanical properties of curved products are, at best, the same as those obtained by conventional extrusion.

Differential velocity sideways extrusion (DVSE), as a novel extrusion-bending-grain-refining process, has been proposed by Zhou et al. (2018a), in which variable curvature can be obtained by using two opposing punches in the extrusion chamber and adjusting their velocity ratio. A further investigation by Zhou et al. (2019) has found this new forming process can lead to greatly refined metallurgical structures in extrudates, due to high values of strains arising in the extrusion orifice. The quantitative relationship between profile curvature and punch velocity ratio has also been determined by FE modelling and upper-bound theorem, as reported by Zhou et al. (2018b). It was found that the curvature obtained by the theoretical model was always greater than that of simulation and experiments due to the die land/bearing length being neglected in the calculations. The curvature discrepancy reveals that in the DVSE process die land length has an obvious effect on the material flow behaviour.

Die land is a very important design factors for extrusion dies because it directly influences the material flow through the orifice, which in turn affects straightness and geometrical defects/quality of the extruded product, as indicated by Chen et al. (2011). Normally, a good design of extrusion die land should make material flow uniform and die strength enough, as pointed out by Ulysse (1999). The effect of die land on material flow is quite complicated, but there are a few useful guidelines, which have been widely employed by the designers for traditional extrusion dies. Castle et al. (1988) proposed that the length of extrusion die land should be proportional to the die orifice width, and a minimum die land length of ~ 2-3 mm is needed to ensure die strength. Zhang et al. (2009) suggested that depending on the extruded workpiece/material property, the length of die land could be ~ 1-3 mm for extrusion of soft metal such as aluminium and copper and ~ 2-4 mm for carbon steel. For the conventional extrusion using one-orifice or multi-orifice die, in which straight profiles are needed, variation of die land length is a common method of controlling flow characteristics through the die orifice, thus most research work on die design has been focused on land length design. Keife (1993) determined the proper land length of a two-orifice flat-faced die based on upper-bound method and conducted plasticine experiments to validate his model. Hao and Li (2000), using a simulation-

adjustment iteration method, suggested a criterion for the judgement of the proper die land of an L-section shape extrusion with a flat-faced die. Lee et al. (2002) numerically investigated the assignment of land lengths in the flat-faced die extrusion process of an L-section. Appropriate die land lengths were assigned to different surfaces of the section to make flow velocity of the workpiece uniform. FE modelling and analytical sensitivity were employed by Ulysse (2002) to achieve an optimal land length of a two-orifice flat-faced die. Ajiboye et al. (2007) utilised the upper-bound theorem to investigate the influence of die land length on the extrusion process of square, rectangular, I-shaped and T-shaped profiles. Ajiboye et al. (2006) also suggested that the length of die land should be greater than or equal to 0.6 of the workpiece diameter for small lead extrudates with negligible bending. Lin and Ransing (2009) proposed a design method for optimising die land length based on minimisation of exit velocity differences of an L-shaped section. Meybodi et al. (2012) developed a general methodology for die land design to avoid bending of the extruded T-shaped profiles, and verified the methodology using experiments of plasticine and FE simulation. Viswanath Ammu et al. (2018) introduced a systematic iterative procedure to optimize die land lengths and achieved uniform velocities across die orifice and a straight unsymmetrical profile. The above research shows that a parallel land over certain length is necessary to extrude straight products. In practice, to obtain straight profiles, die land usually should have sufficient lengths. However, increasing the die land length leads to decrease of the maximum possible extrusion reduction. Large values or significant variations of die land length can also result in defects/failures of the extrudates. For this reason, the die land needs to be carefully designed. Therefore, it is clear that a good design for the proposed DVSE process needs to have a low die land length or land length variation, and the effect of die land on profile curvature and deformation behaviour needs to be investigated.

In this paper, effects of die land length and geometry on curvature and effective strain of profiles produced by DVSE were studied using a novel rig consisting of split extrusion dies and a bi-directional motion loading device. Experiments were carried out with workpieces of plasticine, a commonly utilised physical model material for studying flow behaviour in forming processes which is needed for tool design investigations, as pioneered by Bay et al. (1995). A finite element model was utilised in parallel with experiments to facilitate understanding of die land effect. The findings will highlight optimisation of die design in DVSE and a wide variety of curved profile forming methods whose principles are internal differential material flow.

2. Experiments and modelling

2.1. DVSE tools

The principle of DVSE and design details of the extrusion dies and double-action loading rig are described in Zhou et al. (2018a), here the basics of the process and the equipment used in this work are shown in **Fig. 1**. **Fig. 1a** shows a schematic of DVSE tool and product. The billet/workpiece is pressed simultaneously at both ends in the vertical channel of the container and extrudes through the orifice of the die situated in the side of the container. A curved extrudate profile forms due to the different velocities of upper and lower punches, which induces velocity gradient across the extrudate cross-section. **Fig. 1b** shows extrusion dies. The vertical channel of the container was D_1 = 25.6 mm (diameter) and H_1 = 150 mm (height). The die orifice was circular of diameter D_2. The die land was parallel and the transition from container to die land was by means of sharp corner. The die land length l can be adjusted (2-12 mm) by adding different numbers of shims (1 mm in thickness) to the die orifice, as shown in **Fig. 1b.** Solid circular sections/profiles were extruded and by mounting a circular mandrel of length extending to that of the land, as shown in **Fig. 1b** hollow profiles also were extruded. The mandrel was circular of diameter D_3. The specific geometry parameters of the die orifice and mandrel used can be seen in **Table 1**.

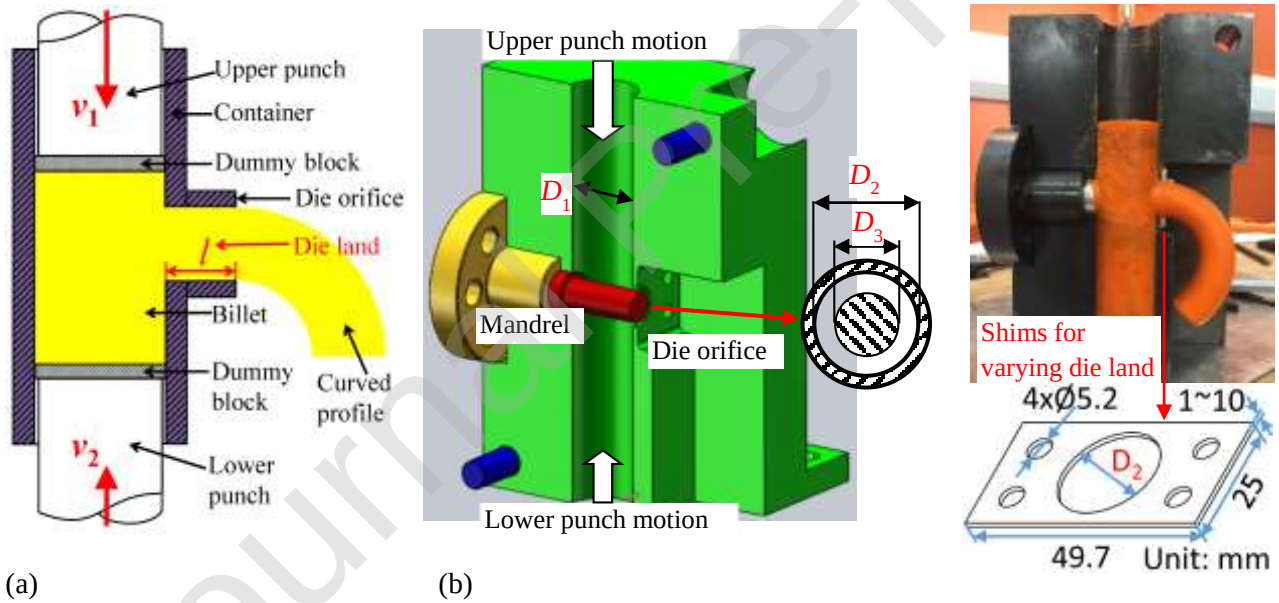

(a) (b)

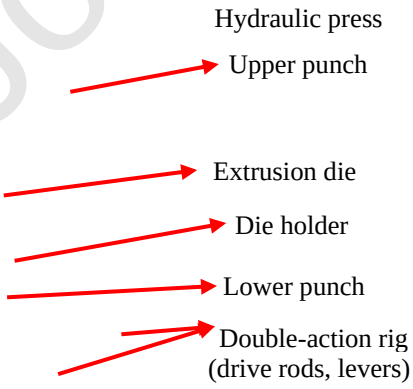

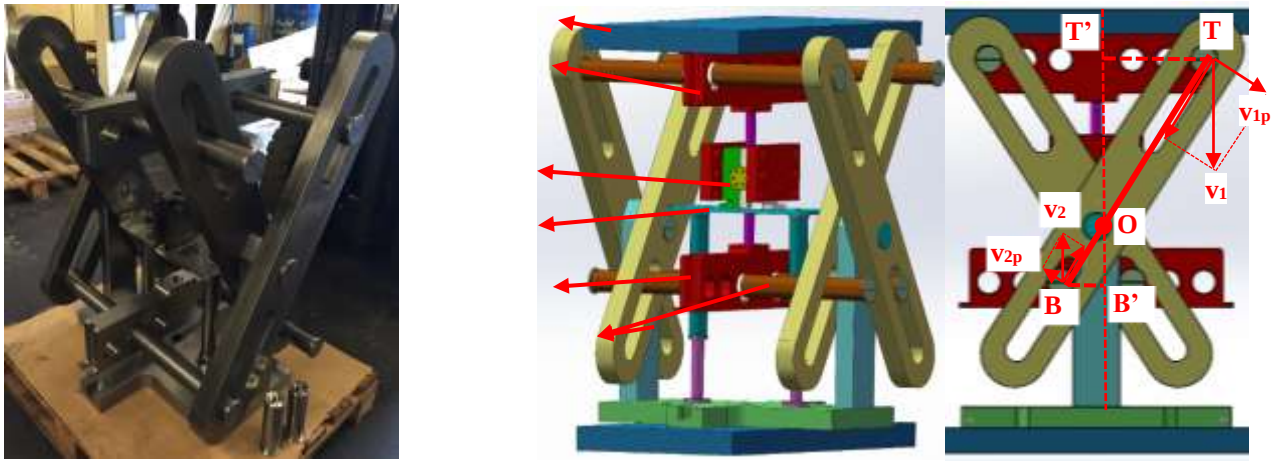

(c) (d)

Fig. 1. (a) Schematic illustration of DVSE process, (b) shims used on split extrusion die for varying die land length, (c) double-action rig and extrusion die assembled, (d) kinematics illustration of the double-action loading rig (Zhou et al., 2018a).

Table 1 Dimensions of the die container, orifice and mandrel used for curved profiles.

	D_1 (mm)	D_2 (mm)	D_3 (mm)	t (mm)	λ
Round bar	25.6	20	-	-	1.61
	25.6	15	-	-	2.87
Round Tube	25.6	15	11	2	6.20

(D_1: die container diameter; D_2: die orifice diameter; D_3: mandrel diameter; t: wall thickness of the extrudate; λ: extrusion ratio)

2.2. Experimental and process modelling details

Plasticine was used as experimental material/workpiece in the DVSE process, which was firstly folded and rolled repeatedly to eliminate possible air pockets and ensure homogeneity. All the workpieces used for extrusion were prepared as cylinders whose diameter and height are 25.4 mm and 130 mm respectively. For extrusion of the hollow extrudates a circular hole of 11 mm diameter was cut along the diameter of a workpiece to contain the mandrel. The extrusion ratio λ of the extrudate is given in **Table 1**. λ is determined by the ratio of the cross-section area of the workpiece to that of the extrudate. Prior to extrusion the plasticine preforms were stored for four days at room temperature to ensure they had attained a steady value of flow stress. The stress-strain data was acquired by compression tests of cylindrical samples with a height of 30 mm and diameter of 25 mm. The compression tests were conducted on a 250 kN Instron hydraulic press at room temperature (23^{o}C). The test strain rates included 0.01, 0.1 and 0.25 s^{-1}. The applied load was recorded by a load cell for each 0.10 mm stroke of the hydraulic press until the sample height reduced to 15 mm. The

true stress-strain curves obtained were fitted as $\bar{\sigma} = 0.181\bar{\varepsilon}^{n_1}\dot{\bar{\varepsilon}}^{n_2}$ MPa, where n_1 = 0.15 and n_2 = 0.14 respectively reflect the strain sensitivity and strain rate sensitivity, $\bar{\varepsilon}$ is the effective strain, $\dot{\bar{\varepsilon}}$ is the effective strain rate. It can be seen that the plasticine used here is a strain-hardening (n_1 = 0.15) and strain-rate-hardening (n_2 = 0.14) viscoplastic material, which is similar to that of many metals at elevated temperatures. For many aluminium alloys and steels, the strain rate sensitivity (n_2) and strain-hardening (n_1) values at elevated temperatures are in the range $0.13 \leq n_2 \leq 0.16$ and $0.10 \leq n_1 \leq 0.25$ (Altan and Boulger, 1973; Xiang et al., 1993; Jiang et al., 2000; El Mehtedi et al., 2015). The strain rate sensitivity of the plasticine (n_2 = 0.14) compares well with that of many aluminium alloys and steels, and its strain-hardening value (n_1 = 0.15) is comparable to those of metals that experience slight strain hardening at elevated temperatures.

Vaseline mixed with soap powder was used as the lubricant during extrusion tests, where a friction factor of 0.3 was determined by ring compression tests (Zhou et al., 2018a). The extrusion experiments were performed on a 2500 kN Instron materials testing press at room temperature (23^{o}C) using the double-action/motion rig (**Fig. 1c**), the mechanism of which is schematically shown in **Fig. 1d** (Zhou et al., 2018a). As can be seen in **Fig. 1d**, the following relationship existed; $v_2/v_1 = v_{2p}/v_{1p}$ = BO/TO = BB'/TT'. For the extrusion of a curved profile, the workpiece was loaded into the container, the punches positioned at its ends and the press operated to drive them into the container. The upper punch velocity v_1 was determined by the velocity of the hydraulic press ram, and the lower punch velocity v_2 depended on the settings of the lever mechanism. In this work the upper punch velocity was 1 mm/s and by adjusting the lever mechanism various velocity ratios v_2/v_1 of; 0, 1/3, 1/2, and 2/3, were used. The die land length l was changeable from 2 mm to 12 mm. At the end of the extrusion process, the two halves of the extrusion tooling were divided apart and the formed shape was extracted to measure its geometry. It should be noted that for the case of $v_2/v_1 < 1$, the upper punch and the lower punch experience different extrusion forces, as has been reported in our previous work (Zhou et al. 2018b). The lack of force equilibrium suggests that there is a high demand for the design of extrusion tool-set, which needs to be properly designed to satisfy the strength requirement and avoid tool failure.

To better understand flow patterns and plastic deformation characteristics a finite element model, containing all elements of the extrusion tooling and workpiece, was constructed using Deform-3D code (Zhou et al., 2018a). The material of the extrusion tooling was considered as rigid and that of the workpiece was plastic, where the elastic deformation was neglected. The physical dimensions of the mandrel and workpiece were the same as that used in experiments. The element type used was tetrahedral element, and the general meshing method was defined by using the absolute mesh density, where 2 was set as the size ratio and 0.5 mm was chosen as the minimum size of an element. Auto-

remesh criteria was set which utilised global remeshing method, a relative interference depth which initiated the remeshing process was set as 0.3, thus remeshing occurred as the element edge penetrated 30% of its previous length. Friction behaviour of the extrusion tooling-workpiece contacting surfaces was modelled with hybrid friction model (Zhou et al., 2018a) $\tau = \begin{cases} mk, & \mu p \geq mk \\ \mu p, & \mu p < mk \end{cases}$, where τ is the friction stress, m is the shear friction factor, $k = \bar{\sigma}/\sqrt{3}$ is the shear yield stress, μ is the Coulomb friction coefficient, and p is the normal pressure on the interface. Here, m = 0.3 was adopted in simulation which was the same as that in experiments, and considering Von-Mises criterion the upper limit of μ = 0.577 m (Ghassemali et al., 2013) were used. FE modelling were carried out using the identical process parameters as those set in the extrusion tests, the modelling results and the test data were then compared.

3. Results and discussion

3.1. Effect of die land length on extrudate curvature

To validate the FE model, flow lines and mesh grids obtained from FEM under different velocity ratios are firstly compared with those from experiments (Zhou et al., 2018a), and the results are shown in **Fig. 2**. The extrusion ratio is λ = 1.61 and the die land length is l = 2 mm. The effective strain is difficult to be quantitatively obtained from experiments, but it can be reflected by the distortion of mesh grids. Extruded solid bars at an extrusion ratio λ of 2.87 with different extrusion/punch velocity ratios and die land lengths, are illustrated in **Fig. 3** and **Fig. 4** shows extruded circular tubes with the same wall thicknesses of 2 mm (that is an extrusion ratio of 6.20) and different extrusion velocity ratios and die land lengths. **Figs. 3-4** also illustrate the related modelling results obtained with FEM. Quantified values for curvature κ are given in **Fig. 5**. **Figs. 2-5** show that there is a good agreement between the FEM and experimental results, thus verifying the modelling results. It should be noted that there are some small differences for the mesh grid distortion. This deviation is inevitably produced since the original (billet) flow lines and mesh grids from experiments (~ 4 mm × 4 mm for coarse grids, ~ 2 mm × 4 mm for fine grids) are manually drawn and are not exactly the same as that accurately made by FEM (4.2 mm × 4.2 mm).

Bending curvature towards the side having a lower extrusion/punch velocity was observed both in the experimental tests and modelling, as shown by the figures. It can also be seen that in most cases the curvatures obtained from the modelling are slightly lower than those acquired from the experiments. Nevertheless, the deviation is not significant, which is presumed as a result of the fact that in experimental tests friction conditions might change with sites, while in the modelling the friction factor/coefficient was regarded as constant. It can be seen that die land length has a significant

effect on curvature, where an 'unbending' or straightening effect on the extrudate is evident. Curvature became lower as the die land length increased, so that varying the die land length altered the material flow state at the die orifice, thus affecting extrudate curvature. For the case of $v_2/v_1 = 0$, the linear approximation values of the curvature results for λ = 2.87 and 6.20 shown in **Fig. 5** are extrapolated to $\kappa = 0$ around $l \sim 12$ mm and 13 mm, respectively. For the case of $0 < v_2/v_1 < 1$, the corresponding l leading to $\kappa = 0$ is less than that of $v_2/v_1 = 0$, which are $l \sim 10$ mm for λ = 2.87, v_2/v_1 = 1/2 and $l \sim 12$ mm for λ = 6.20, v_2/v_1 = 1/3, respectively.

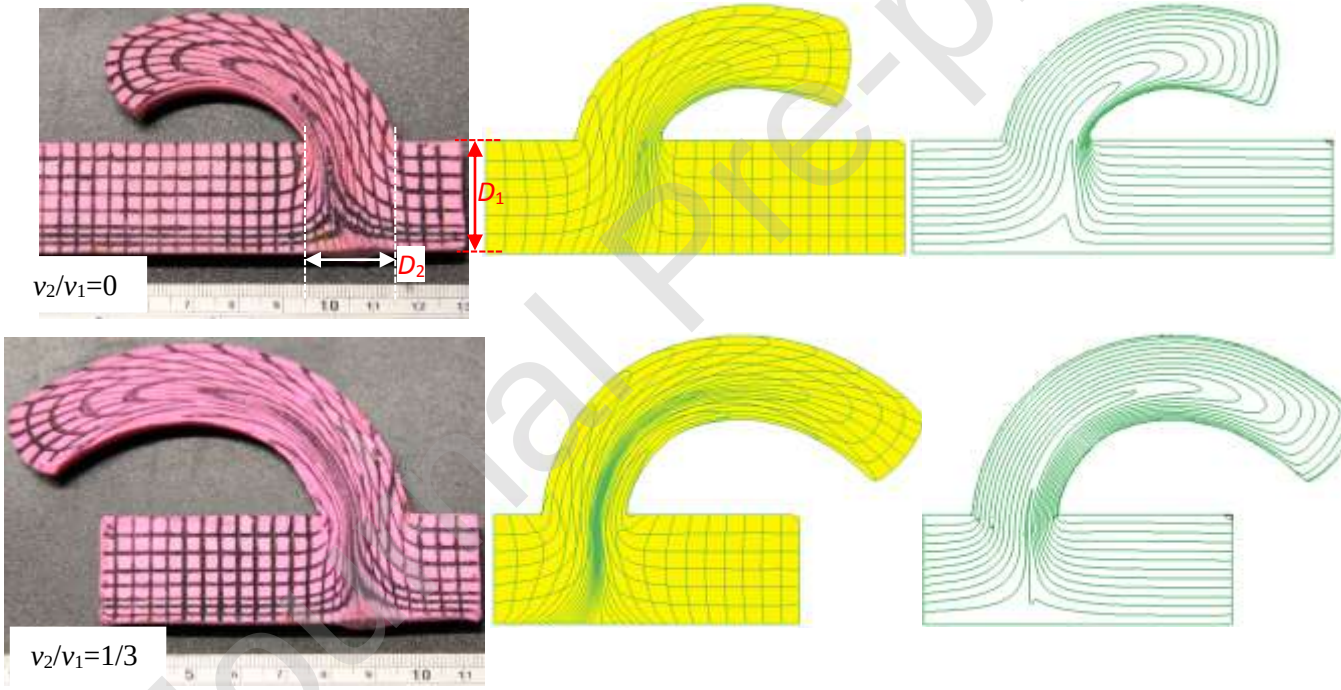

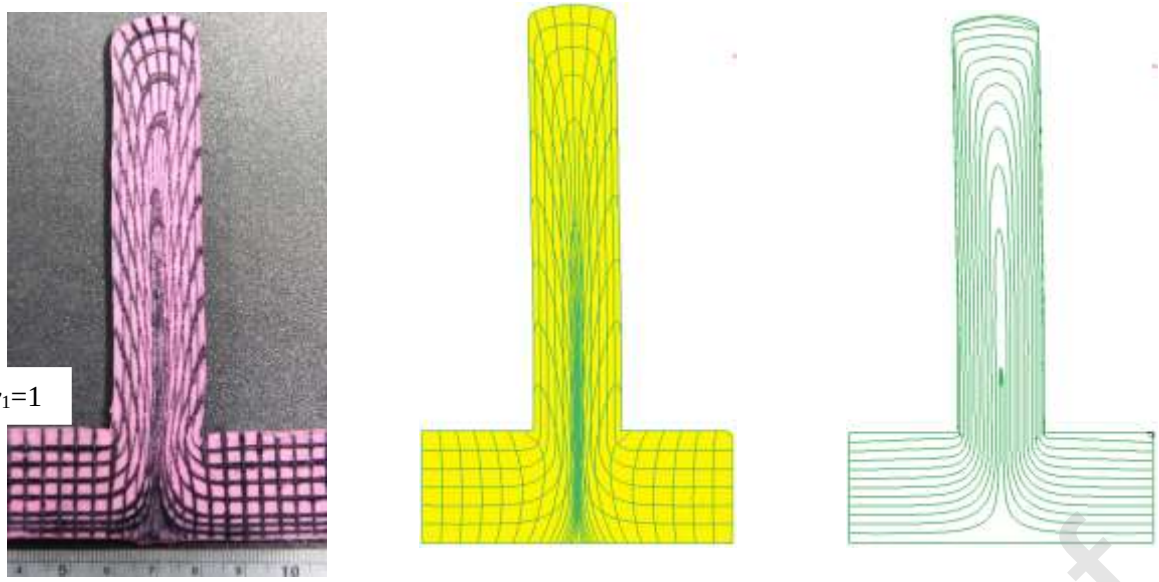

Fig. 2. Comparison of flow lines and mesh grid distortion obtained from experiments and FEM.

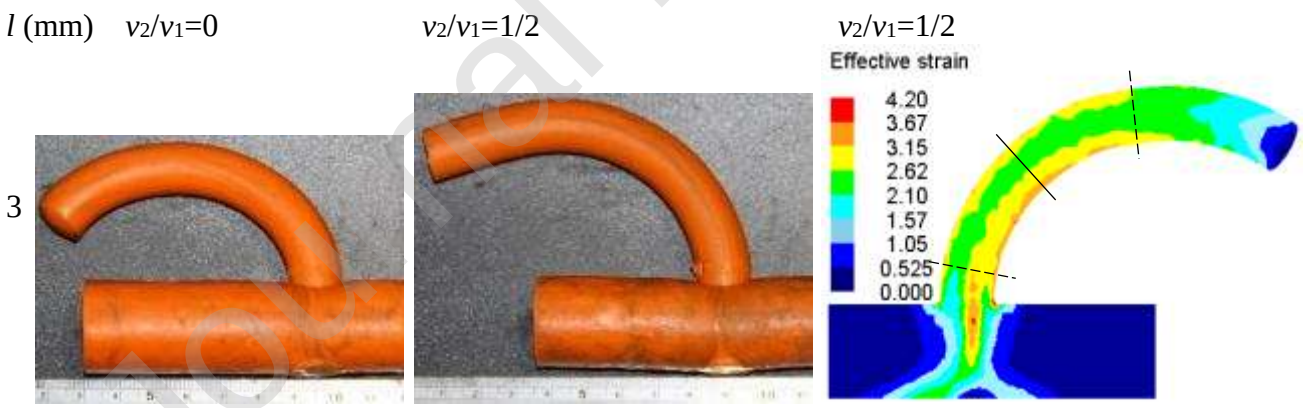

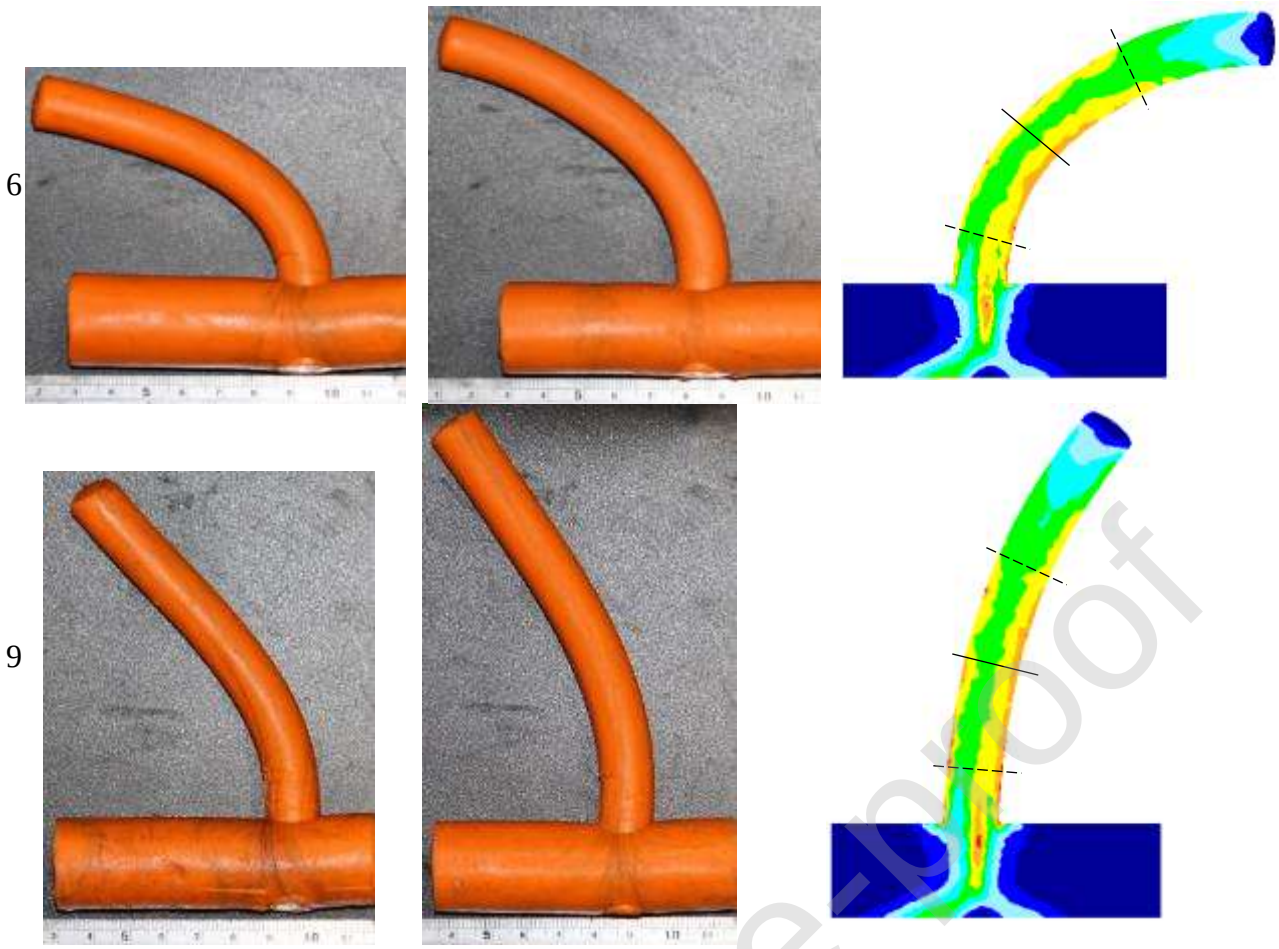

Fig. 3. Solid bars extruded at λ = 2.87, v_2/v_1 = 0, 1/2, and die land length l = 3, 6, 9 mm: (a) experiment, (b) FEM

l (mm) v_2/v_1=0 v_2/v_1=1/3 v_2/v_1=1/3

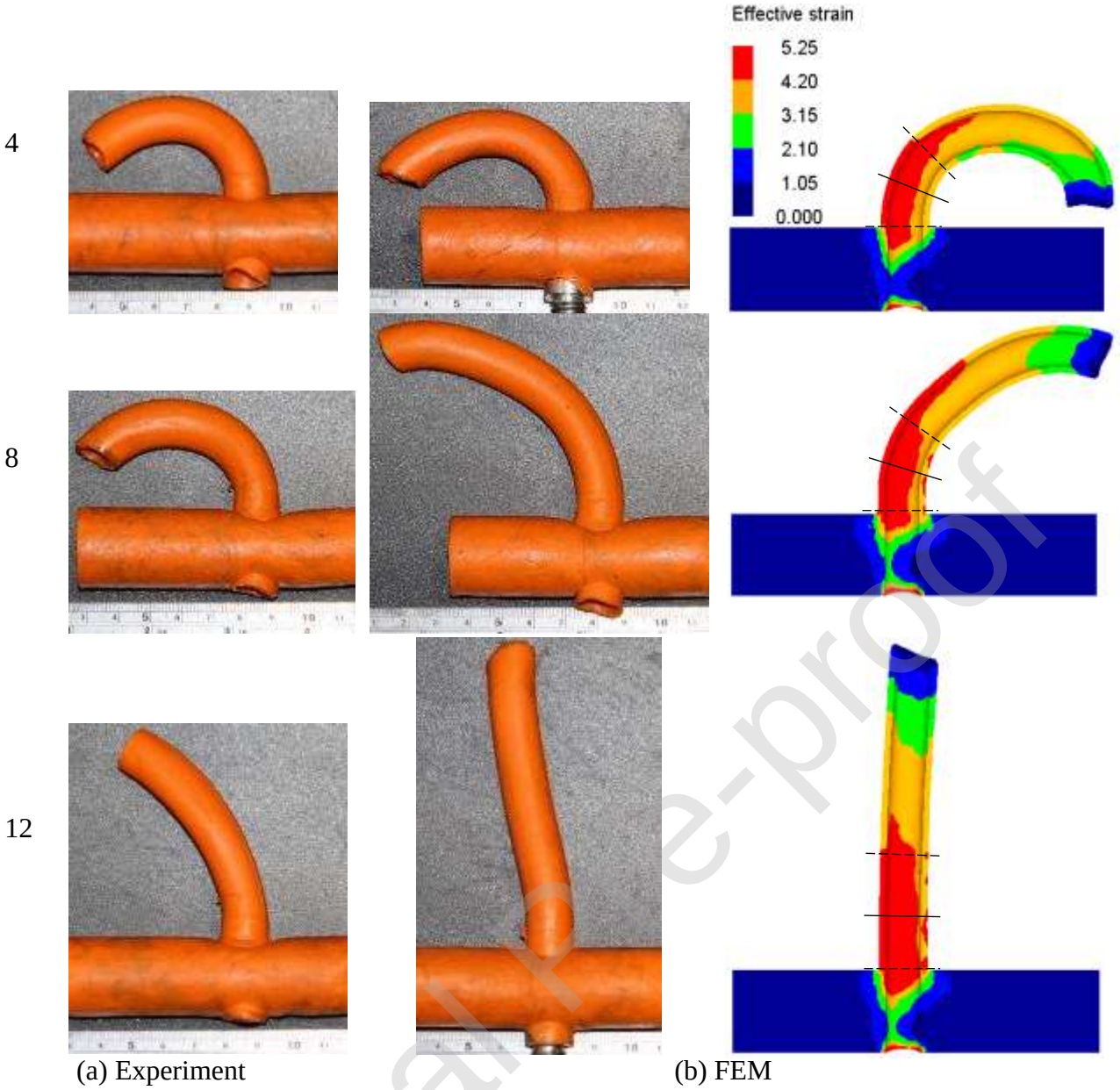

Fig. 4. Tubes extruded at λ=6.20 (thickness 2 mm), v_2/v_1=0, 1/3, and die land length l = 4, 8, 12 mm: (a) experiment, (b) FEM

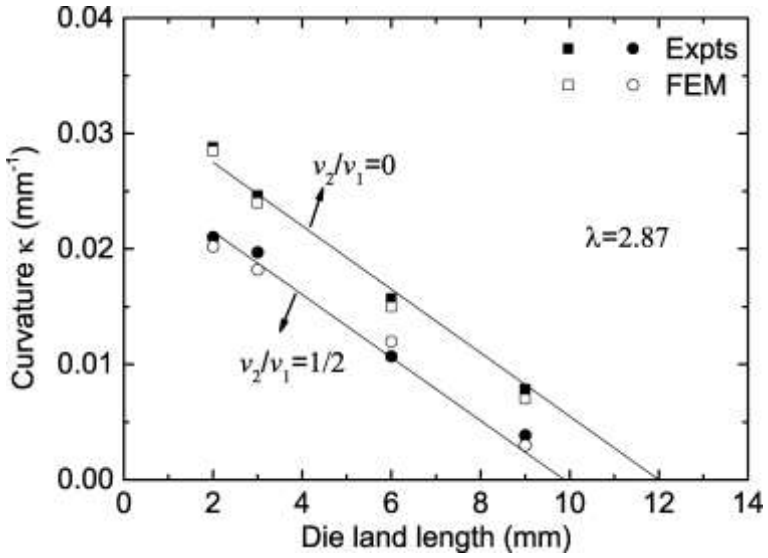

(a) Solid bars

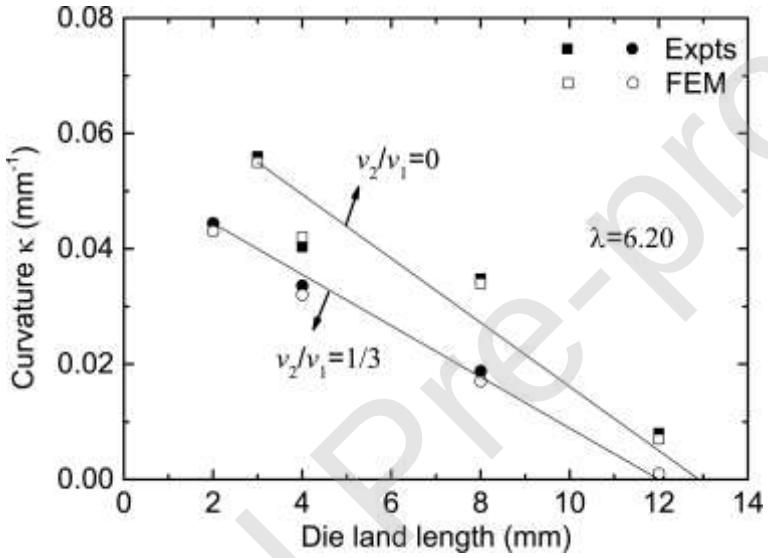

(b) Tubes

Fig. 5. Quantified values for curvature κ obtained from experiment (solid symbols) and modelling (hollow symbols) for different die land lengths: (a) solid bars, (b) tubes.

The straightening effect of die land on profile curvature has also been found in the processes of equal channel angular extrusion/pressing (ECAE/P) (Li et al., 2010) and in curved profile extrusion using an inclined die orifice (Takahashi et al., 2015), a critical ratio of die land length to profile diameter has been found beyond which the velocity difference over the die exit orifice is compromised resulting in straight profiles. This critical ratio was between 0.5-2 (Li et al., 2010) for ECAE/P and about 1 (Takahashi et al., 2015) for curved profile extrusion with a 30° inclined die orifice. The ECAE/P process could be regarded reasonably as a special case of DVSE with λ = 1 and v_2/v_1 = 0, the ratio of the exit channel length (die land length) to entry/exit channel diameter (profile diameter) in all ECAE/P practise falls within or is larger than 0.5-2 so that the flow velocity difference across the exit channel orifice caused by the unidirectional extrusion/pressing v_1 is compromised and straight

extrudate is obtained. In DVSE, the die land length should be as small as possible to decrease its effect on the material flow difference at die exit orifice which is deliberately caused by the opposing punches with different velocities.

The influence of die land length on profile curvature is because the material flow state at the die orifice is affected by the die land length, which is further investigated through flow field simulation at the die land. A comparison of velocity distribution at the die orifice for round bars extruded with different die land lengths is illustrated in **Fig. 6**. The extrusion ratio and velocity ratio in **Fig. 6a-b** are the same and are $\lambda = 2.87$ and $v_2/v_1 = 0$, respectively. As can be seen in **Fig. 6a**, for die land length of 1 mm, material flow velocity at the orifice upper edge (extrados) which is closer to the faster upper moving punch is at 4.6 mm/s (line H), it is lower at the orifice lower edge (intrados) which is at 1.9 mm/s (line A). For the greater land length of 3 mm, as can be seen in **Fig. 6b**, material flow velocity is reduced to 3.75 mm/s (line H) at the orifice upper edge (extrados) and decreased towards the orifice lower edge (intrados) which is at 2.3 mm/s (line A). Thus it is demonstrated that die land has an 'unbending' or straightening effect on the extrudate; greater die land length leads to a decreased velocity gradient across the die orifice and thereby lower profile curvature.

(a) l = 1 mm, λ=2.87, v_2/v_1=0 (b) l = 3 mm, λ=2.87, v_2/v_1=0

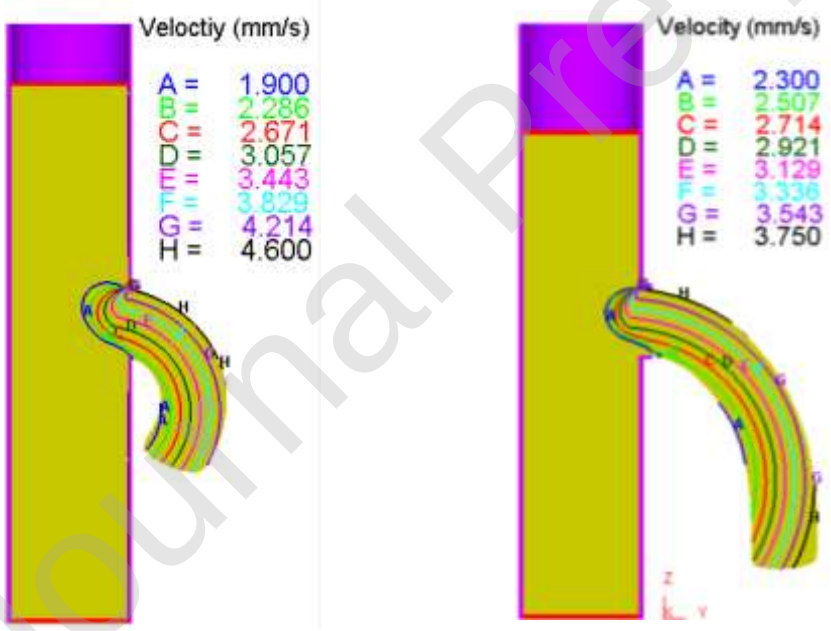

Fig. 6. Influence of die land length on material flow.

The profile curvature under different land ratios has been calculated, where the land ratio l_λ is defined as the length l of die land normalized by die orifice diameter D_2:

$$l_\lambda = l/D_2 \tag{1}$$

For the case of $v_2/v_1 = 0$, the linear approximation values of the curvature results for λ = 1.61, 2.87 and 6.20 are extrapolated to $\kappa = 0$ giving values of l_λ of about, 0.76, 0.80 and 0.86, respectively. For the case of $0 < v_2/v_1 < 1$, the corresponding values of l_λ leading to $\kappa = 0$ are, $l_\lambda = 0.63$ for $\lambda = 1.61$, $v_2/v_1 = 1/2$, $l_\lambda = 0.66$ for $\lambda = 2.87$, $v_2/v_1 = 1/2$, and $l_\lambda = 0.80$ for $\lambda = 6.20$, $v_2/v_1 = 1/3$, respectively, which are all less than that for $v_2/v_1 = 0$. From examination of this data it is inferred that profile curvature is APPENDIX

ressed by the material flow near the die orifice as a result of the effect of the land ratio l_λ over a critical value l_0. To explore the relation between l_0, λ and v_2/v_1, l_0 was computed from a series of FE modelling trials with different process parameters (extrusion ratios and extrusion velocity ratios). As can be seen in **Fig. 7a**, l_0 increased approximately exponentially with increase in extrusion ratio. For the limiting case of $v_2/v_1 = 0$, the relation between l_0 and extrusion ratio λ was found to be

$$l_0 = c\lambda^n \tag{2}$$

where c = 0.731, n = 0.086. **Fig. 7a** also shows that the value of l_0 depends on extrusion velocity ratio. It is shown in **Fig. 7b** that l_0/λ^n decreases approximately exponentially with increase of v_2/v_1 for different extrusion ratios. Thus:

$$l_0/\lambda^n = f(v_2/v_1) \tag{3}$$

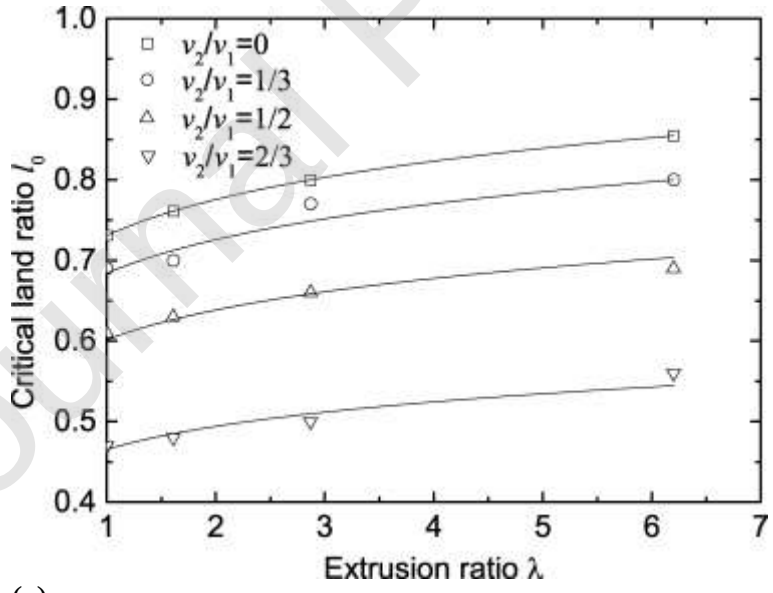

(a)

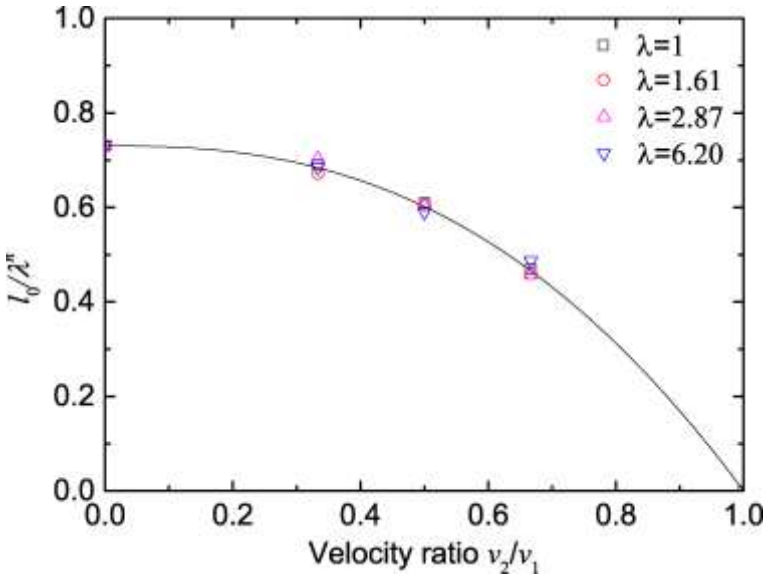

(b)

Fig. 7. (a) Relation between l_0 and λ, v_2/v_1, (b) relation between l_0/λ^n and v_2/v_1.

For the case of $v_2/v_1 = 0$, we have

$$c = f(v_2/v_1 = 0) \tag{4}$$

The relation between the l_0/λ^n and velocity ratio has been fitted as:

$$\frac{l_0}{\lambda^n} = f\left(\frac{v_2}{v_1}\right) = c\left[1 - \left(\frac{v_2}{v_1}\right)^m\right] \tag{5}$$

where m = 2.50. It can be seen that as v_2/v_1 approaches 1, the more rapidly l_0 approaches 0. For the ideal case $v_2/v_1 = 1$, l_0 could be infinitely small for all extrusion ratios, in theory and disregarding lack of die strength.

3.2. Effect of die land length on extrudate effective strain

The effective strain in solid bars (λ = 2.87, v_2/v_1 = 1/2) for different die land lengths (l = 3, 6, 9 mm) is given pictorially in **Fig. 3** and **Fig. 4** illustrates pictorially the effective strain in tubes (λ = 6.20, v_2/v_1 = 1/3) for different die land lengths (l = 4, 8, 12 mm). It can be seen that a relatively high level of plastic strain has been induced in the DVSE process. The intrados region of the bar has the highest local plastic deformation, and effective strain gradually decreases towards centre before increasing towards the extrados. The region near extrados of the tube has the highest local plastic deformation due to its interaction with the mandrel. Although curvature decreases as the length of die land increases, it is noticed that the effect of die land length on overall effective strain level was not pronounced, especially for that of the bar. Only the surface layers which contact with die land and mandrel (for tube inner surface) appear to have an increase in strain as die land length increases.

To further understand the effect of die land length on deformation behaviour, flow lines were scribed on undeformed workpieces, which were then extruded at different die land lengths (l = 3, 6, 9 mm). As can be seen in **Fig. 8**, DVSE could be regarded reasonably as two non-equal channel angular pressing/extrusion (N-ECAP/E) processes, where e denotes the distance between the boundary extension line of the die orifice edge (near the faster moving punch) and the dividing line, D_2 denotes the die orifice diameter (Zhou et al., 2018a). As the workpiece in the extrusion container is extruded through the intersection planes ('V' shape) of the two channels (entry D_1, exit $(D_2 - e)$ or e), the material flow direction is altered by 90 degree due to the action of strong shearing (Zhou et al., 2019). Effective strain is closely related to effective extrusion ratio which is affected by the eccentricity ratio

$$\xi = e/D_2 \tag{6}$$

where $0.5 \leq \xi < 1$ is a normalised dimensionless variable. The influence of die land length on e or the eccentricity ratio ξ is shown in **Fig. 8**. As die land length has little effect on eccentricity ratio, its effect on the overall effective strain level is limited. However, strain inhomogeneity is different under different lengths of die land for a given velocity ratio.

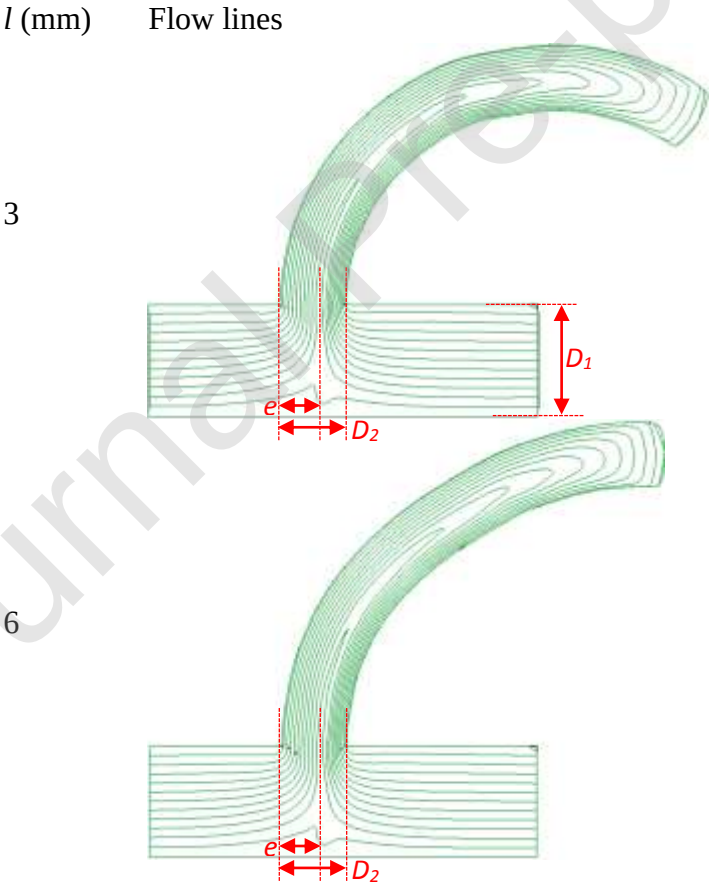

9

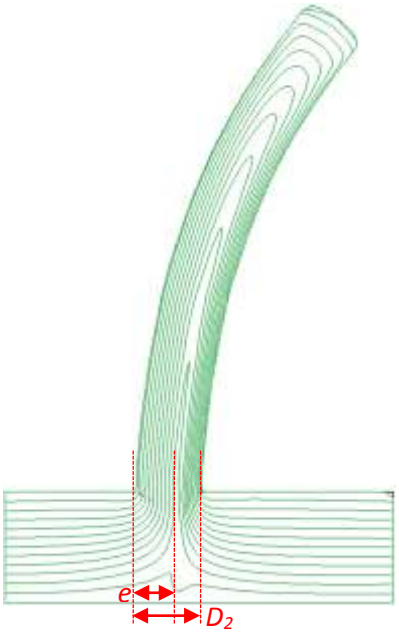

Fig. 8. Influence of die land length on flow lines for bars extruded at λ = 2.87, v_2/v_1 = 1/2, and die land length l = 3, 6, 9 mm.

Two methods were used to quantify the degree of strain inhomogeneity. The first was using inhomogeneity index (C_i) proposed by Li et al. (2004):

$$\bar{\varepsilon}_{Ci} = \frac{\bar{\varepsilon}_{max} - \bar{\varepsilon}_{min}}{\bar{\varepsilon}_{avg}} \tag{7}$$

where $\bar{\varepsilon}_{max}$, $\bar{\varepsilon}_{min}$ and $\bar{\varepsilon}_{avg}$ are maximum, minimum and average values of effective strain $\bar{\varepsilon}$, respectively. Average value of effective strain in the cross-section is obtained by

$$\bar{\varepsilon}_{avg} = \frac{\sum_{j=1}^{N} \bar{\varepsilon}^j}{N} \tag{8}$$

where $\bar{\varepsilon}^j$ is the effective strain of the node j and N is the total number of nodes of the cross-section. Another is a mathematical coefficient named coefficient of variance (C.V.), C.V. of the effective strain is defined as (Basavaraj et al., 2009):

$$\bar{\varepsilon}_{CV} = \frac{\bar{\varepsilon}_{SD}}{\bar{\varepsilon}_{avg}} \tag{9}$$

where $\bar{\varepsilon}_{SD}$ is standard deviation (S.D.) of the effective strain $\bar{\varepsilon}$, which is expressed as

$$\bar{\varepsilon}_{SD} = \sqrt{\frac{\sum_{j=1}^{n} (\bar{\varepsilon}^j - \bar{\varepsilon}_{avg})^2}{N}} \tag{10}$$

As the workpiece being extruded out of the die orifice, the strain distribution begins to stabilize. Increase the extrusion stroke will lead to an increase in this part of the steady-state region. As shown in **Figs. 3-4** as a solid line, a cross-section in this part is taken into account to calculate strain

inhomogeneity. **Fig. 9** illustrates variations of effective strain over the selected cross-section extracted from modelling. The calculated values of inhomogeneity index (ε_{Ci}) and coefficient of variance (ε_{CV}) of effective strain are given in **Table 2**. It is clear from **Table 2** that die land length has less effect on the strain level of bars than of tubes, especially for the centre region. But its effect on the strain inhomogeneity is obvious. Both ε_{Ci} and ε_{CV} indicate that the inhomogeneity is lower in case of smaller die land length for bars. The influence of die land length on the effective strain is most obvious for the surface layers. They have a greater effective strain for longer die land length, resulting in decreased strain homogeneity over the cross-section of bars. This is because of the greater surface shear force resulting from the greater frictional areas of longer length die lands. For tubes, as both the mandrel and die land have frictional areas, the effect of die land length on strain level is more obvious than for bars, but its effect on the strain inhomogeneity is more complicated and is related to wall thickness. For the 2 mm wall thickness (see **Fig. 9b)**, as die land length increases, in addition to innermost and outermost surface layers which have increased effective strain similar to that of bars, the effective strain of the entire wall has increased due to its relatively small thickness. Strain inhomogeneity of the tube along the selected path (cross-section) is given in **Table 2**. Generally, as die land length increases, both the extrados wall (AB) and intrados wall (CD) have an increased strain inhomogeneity, while the innermost surface (BC) has a decreased inhomogeneity, leading to a decreased strain inhomogeneity along the entire selected path (AD).

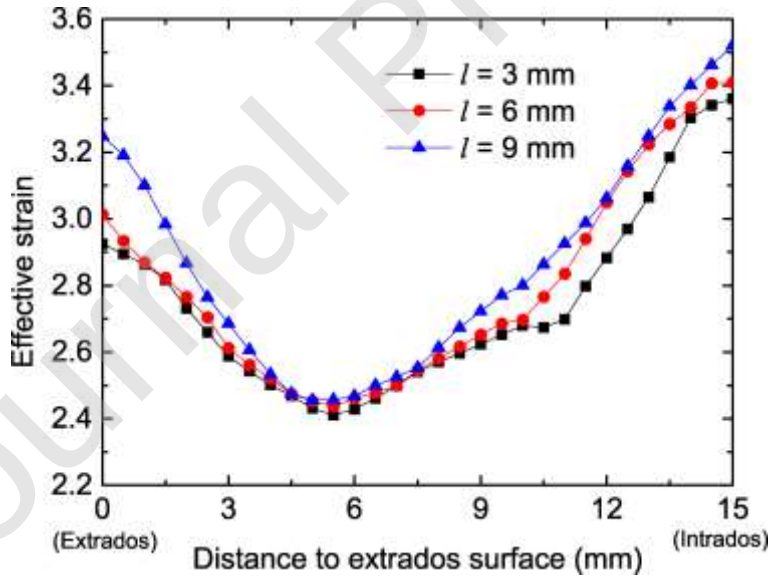

(a) Solid bars

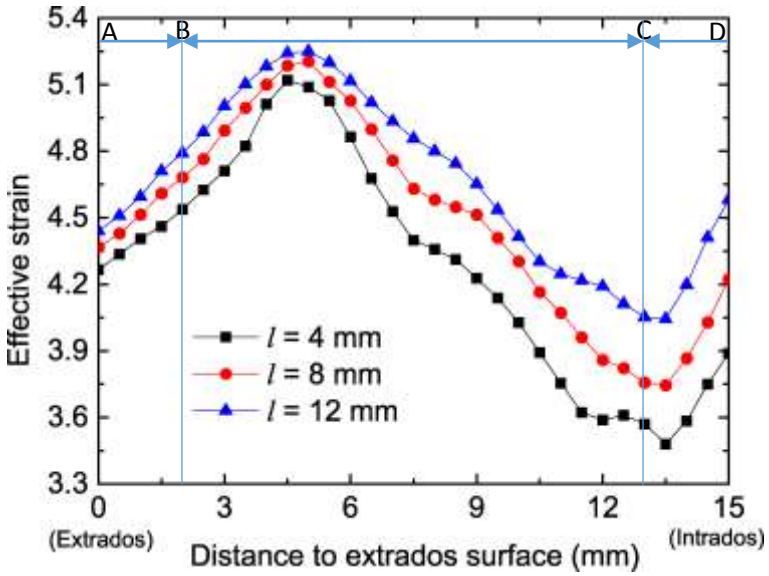

(b) Tubes

Fig. 9. Effective strain distribution in the selected cross-section: (a) round bars, (b) tubes.

Table 2 Inhomogeneity index (ε_{Ci}) and coefficient of variance (ε_{CV}) of effective strain

v_2/v_1	1/2 (Bar)			1/3 (Tube)								
Die land (mm)	3	6	9	4			8			12		
				AB	CD	AD	AB	CD	AD	AB	CD	AD
ε_{avg}	2.747	2.799	2.870	4.401	3.654	4.280	4.520	3.924	4.484	4.609	4.257	4.656
ε_{Ci}	0.346	0.347	0.371	0.061	0.112	0.383	0.069	0.122	0.325	0.076	0.126	0.259
ε_{CV}	0.100	0.108	0.115	0.024	0.045	0.118	0.028	0.052	0.100	0.031	0.055	0.081

3.3. Effect of die land geometry on extrudate curvature

Research has shown that for ECAE/P or N-ECAE/P, in addition to die land length (outlet channel length) (Li et al., 2010), die land geometry or outlet channel geometry has an effect on the deformation behaviour of extrudate (Basavaraj et al., 2009). This section seeks to explore geometry of die land/container transition corner through the viewpoint of curvature and strain behaviour. Three different transition corners of die land geometry studied are shown in **Fig. 10**, which in **Fig. 10a** is sharp, in **Fig. 10b** chamfered, and in **Fig. 10c** radiused.

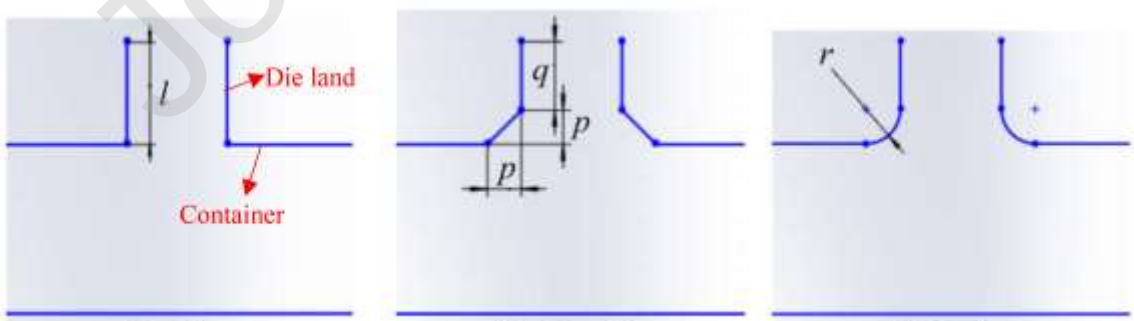

(a) Sharp (b) Chamfer (c) Radius

Fig. 10. Die land/container transition corner geometries: (a) sharp, (b) chamfered, (c) radiused.

Four different cases were simulated for die land length l = 3 mm and extrusion ratio λ=2.87; (i) sharp, l = 3 (p = 0, q = l), (ii) chamfer 1 mm, p = 1, q = 2, (iii) chamfer 2 mm, p = 2, q = 1, (iv) radius 2 mm, r = 2 (q = 1), where p is corner parameter, q is the effective parallel land length. Values of p and q have a relation with that of die land length l as $l = p + q$. Effects of both velocity ratios v_2/v_1 = 0 and 2/3 have been studied and the results are illustrated in **Fig 11.** It is clear from **Fig. 11** that die land/container transition corner geometry has an effect on profile curvature. **Fig. 12** illustrates the specific values of profile curvature. As shown in **Fig. 12,** it is clear that for both velocity ratios of v_2/v_1 = 0 and 2/3, curvature resulting from a chamfered or radiused transition is greater compared with that resulting from a sharp transition, and curvature resulting from a 2 mm chamfer is greater than that from a 1 mm chamfer. The increase in curvature is attributed to the decreased effective die land length, which in cases (ii)-(iv) is smaller than that in case (i). Furthermore, the effective land length in case (iii) is smaller than that in case (ii). For the same category of die corner, the effect of effective land length on curvature decreases as velocity ratio v_2/v_1 increases, as can be seen in **Fig. 12** that the difference in curvature resulting from a 2 mm chamfer and 1 mm chamfer is greater for velocity ratio of v_2/v_1 = 0 than that of v_2/v_1 = 2/3. For a chamfered land corner (case (iii)) and a radiused corner (case (iv)) with the same effective die land length, the curvature in case (iii) is greater than that in case (iv) for velocity ratio of v_2/v_1 = 0, whereas for v_2/v_1 = 2/3 the curvature in case (iii) is slightly smaller than that in case (iv). This might be because the effect of die land transition geometry on material flow is more complicated for double-sided extrusion (v_2/v_1 = 2/3) than for one-sided extrusion (v_2/v_1 = 0). Generally, the difference in curvature resulting from a chamfered and radiused land corner with the same effective land length decreases as velocity ratio v_2/v_1 increases.

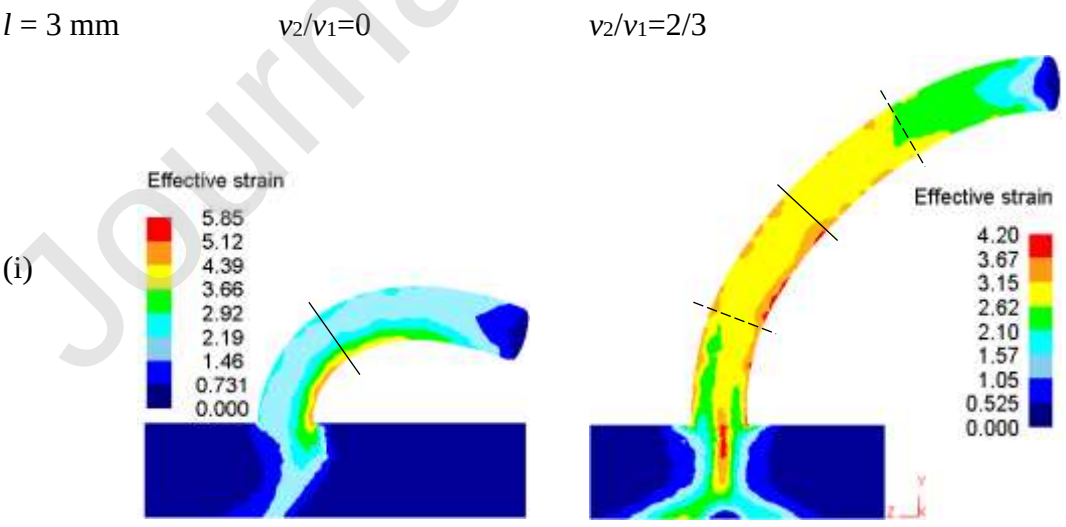

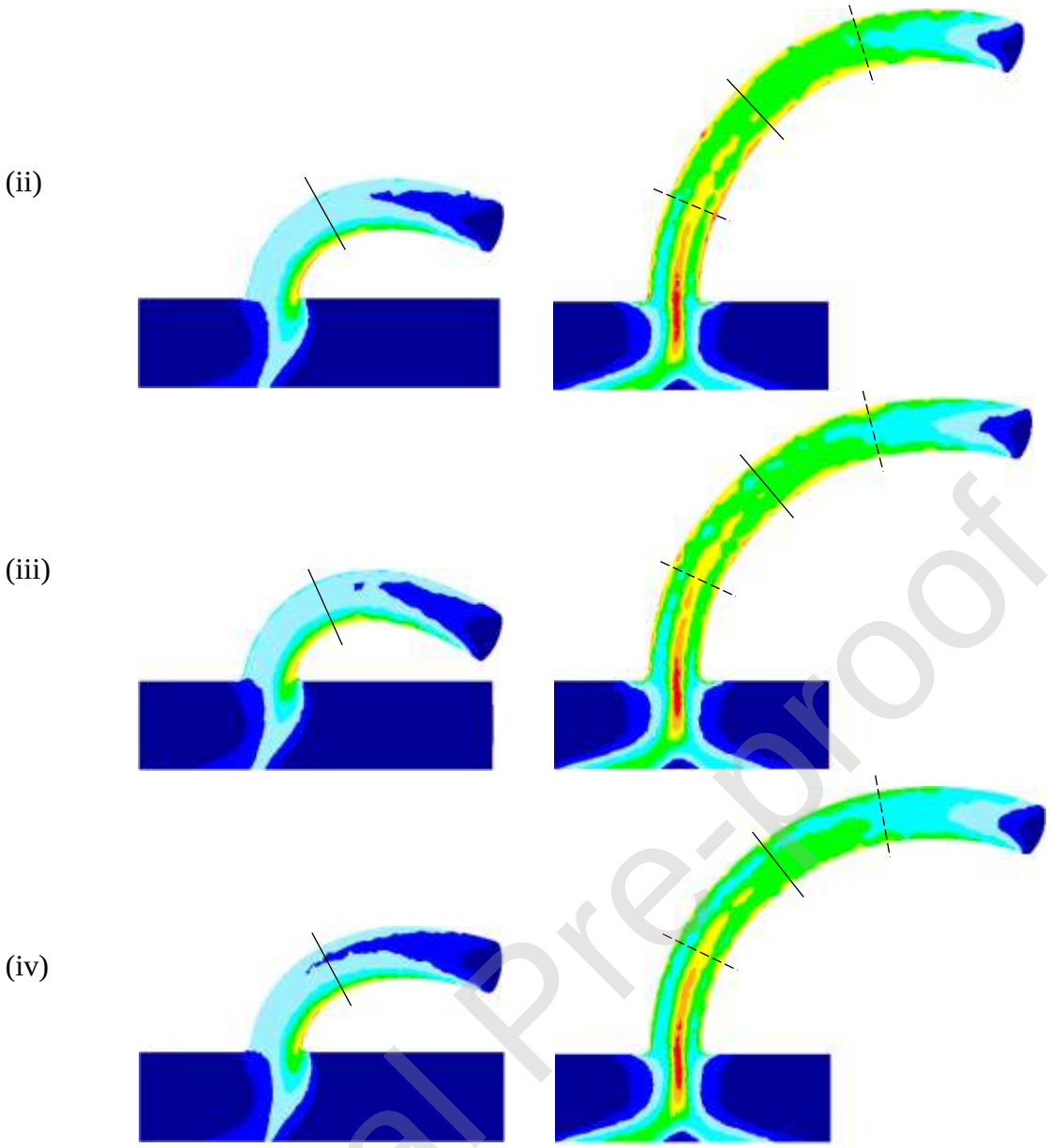

Fig. 11. Profile curvature and effective strain for container/orifice transition corners: (i) sharp, (ii) chamfer 1 mm, (iii) chamfer 2 mm and (iv) radius 2 mm, for velocity ratios of $v_2/v_1 = 0$, and 2/3.

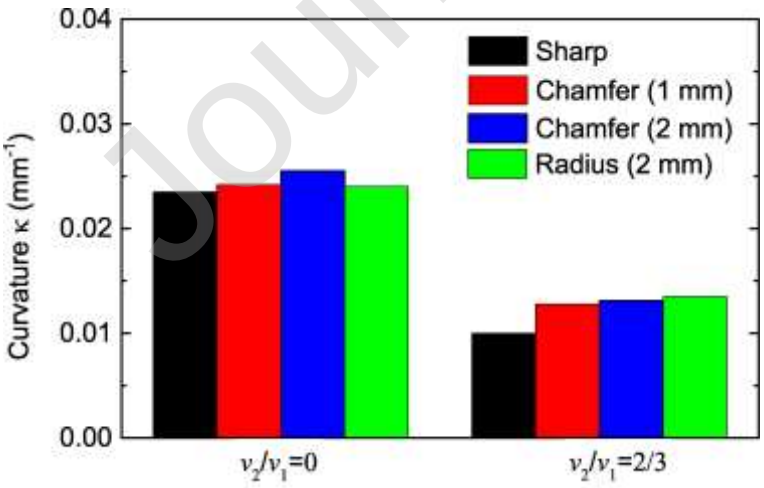

Fig. 12. Specific value of profile curvature.

3.4. Effect of die land geometry on extrudate effective strain

Fig. 13 shows the effective strain distribution in the selected extrudate cross-section (shown as solid line in **Fig. 11**). The average effective strain ε_{avg}, strain inhomogeneity ε_{CV}, ε_{Ci} are given in **Table 3**. For different cases, the cross-section was selected at the same location of the profiles (corresponding to the same stroke). It can be seen that there is a considerable effect on the overall strain and strain homogeneity. The average effective strain gradually decreases from case (i) to case (iv), with the radiused corner leading to the smallest effective strain level. It should be noted that for v_2/v_1 = 2/3 and λ = 2.87, we have ξ ~ 0.53 (Zhou et al., 2018a), thus the dividing line defined by Eq. (6) is at e ~ 8 mm. From the position of extrados surface layer towards the dividing line, the effective strain is relatively large at surface layer due to zone of shear along the profile surface being generated. It decreases as the location is away from the surface layer, however it will slightly increase when the location is close to the dividing line. This is probably due to the interaction of the material coming oppositely at the boundary (dividing) line from left and right parts. As $\xi D_2 > (1-\xi)D_2$, the right part with the sectional width $(1-\xi)D_2$ has greater effective extrusion ratio than the left part with the sectional width ξD_2. Therefore, the right part (intrados) of the curved profile closer to the slower moving punch has a greater effective strain than the left part (extrados). Generally, the effective strain is most severe for the sharp corner and in comparison; a profiled corner decreases effective strain over the entire cross-section especially for the region between the dividing line and the extrados/intrados surface layer, leading to a decreased average effective strain level. To achieve a relatively homogenous and high value effective strain, a sharp cornered transition is recommended.

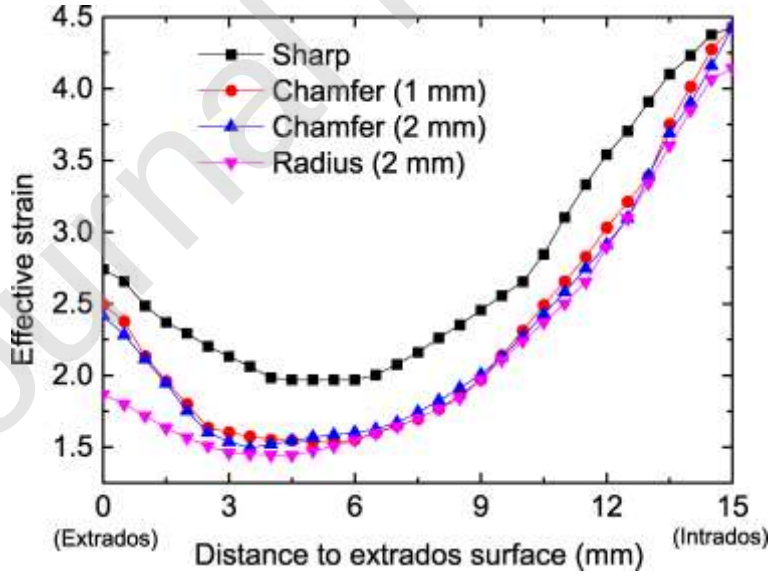

(a)

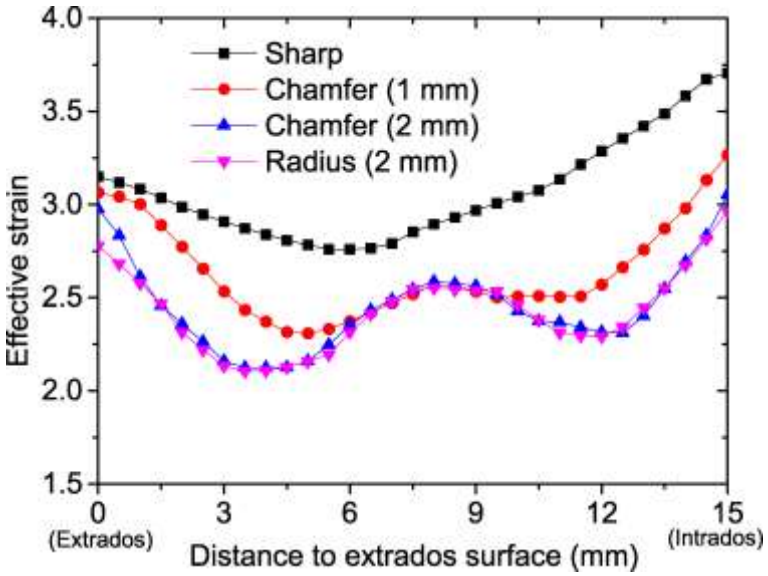

(b)

Fig. 13. Effective strain distribution in the selected cross-section: (a) v_2/v_1=0, (b) v_2/v_1=2/3.

Table 3 Inhomogeneity index (ε_{Ci}) and coefficient of variance (ε_{CV}) of effective strain

v_2/v_1	0				2/3			
	Sharp	Chamfer 1mm	Chamfer 2mm	Radius	Sharp	Chamfer 1mm	Chamfer 2mm	Radius
ε_{avg}	2.739	2.335	2.306	2.187	3.072	2.643	2.457	2.430
ε_{Ci}	0.898	1.240	1.272	1.234	0.308	0.362	0.377	0.354
ε_{CV}	0.293	0.375	0.368	0.388	0.089	0.100	0.098	0.090

To further provide an understanding of the effect of die land geometry on the plastic deformation behaviour, **Fig. 14** illustrates the effective strain rate across the deforming region obtained from modelling for the above four cases with extrusion ratio λ = 2.87 and velocity ratio v_2/v_1 = 2/3. It can be seen from **Fig. 14** that effective strain rate decreases from the corners of the die orifices through an arc, across the deforming region. The maximum effective strain rate distributions are focused around the two intersection planes ('V' shape) of the two channels (D_1 and ξD_2, D_1 and $(1-\xi)D_2$, respectively). It should be noted that the scale in these figures have been manually adjusted to highlight the strain rate within the intersection region and the strain rate in the die orifice corner is much larger than the maximum value shown in these figures.

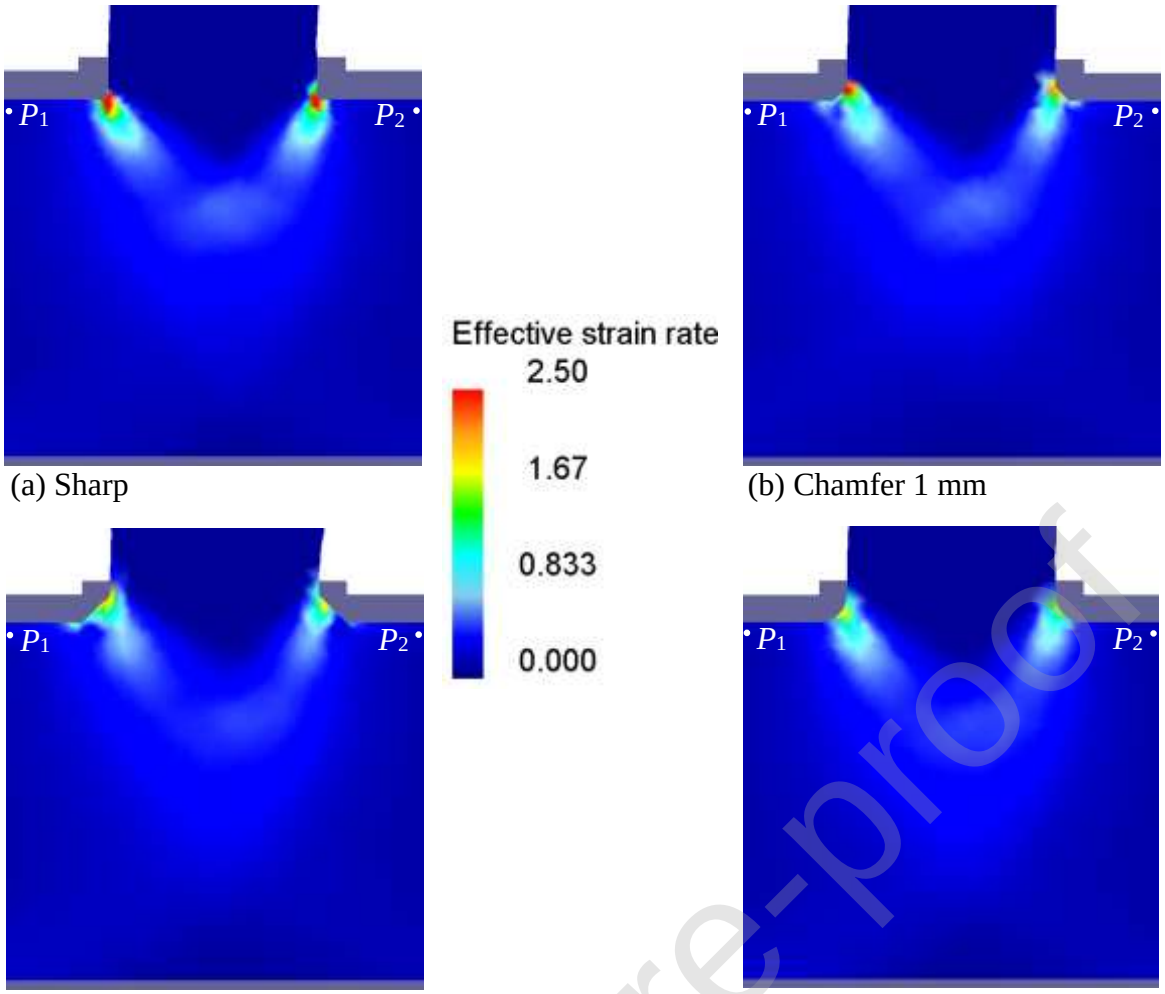

(a) Sharp (b) Chamfer 1 mm

(c) Chamfer 2 mm (d) Radius 2 mm

Fig. 14. Effective strain rate contours for different die land transition corners: (a) sharp, (b) chamfer 1 mm, (c) chamfer 2 mm, (d) radius 2 mm.

Two points near each side of the workpiece surface (~ 0.75 mm depth and P_1P_2 = 30 mm mutual distance, P_1 on the side with punch velocity v_1, P_2 on the side with punch velocity v_2) were chosen to trace the evolution of effective strain rate with time, as illustrated in **Fig. 14**, and the results are given in **Fig. 15**. The effective strain accumulated along a flow line incorporating point P_i can be obtained if the effective strain rate $\dot{\bar{\varepsilon}}(P_i)$ was multiplied by the deformation time t, which was calculated through integration in **Fig. 15** as:

$$\bar{\varepsilon}(P_i) = \int_t \dot{\bar{\varepsilon}}(P_i)dt \tag{11}$$

The calculated effective strains $\bar{\varepsilon}(P_1)$ and $\bar{\varepsilon}(P_2)$ are given in **Fig. 15**. It can be seen that a chamfer or radius leads to significantly decreased strain rates. Effective strain is most severe for the sharp corner, where zones of narrow and intense shear exist on the intersection planes ('V' shape) of the deforming region shown in **Fig. 14**. These zones of shear along the intersection planes are found to be much dispersed and weaker for the die land with a profiled corner, especially a radiused one.

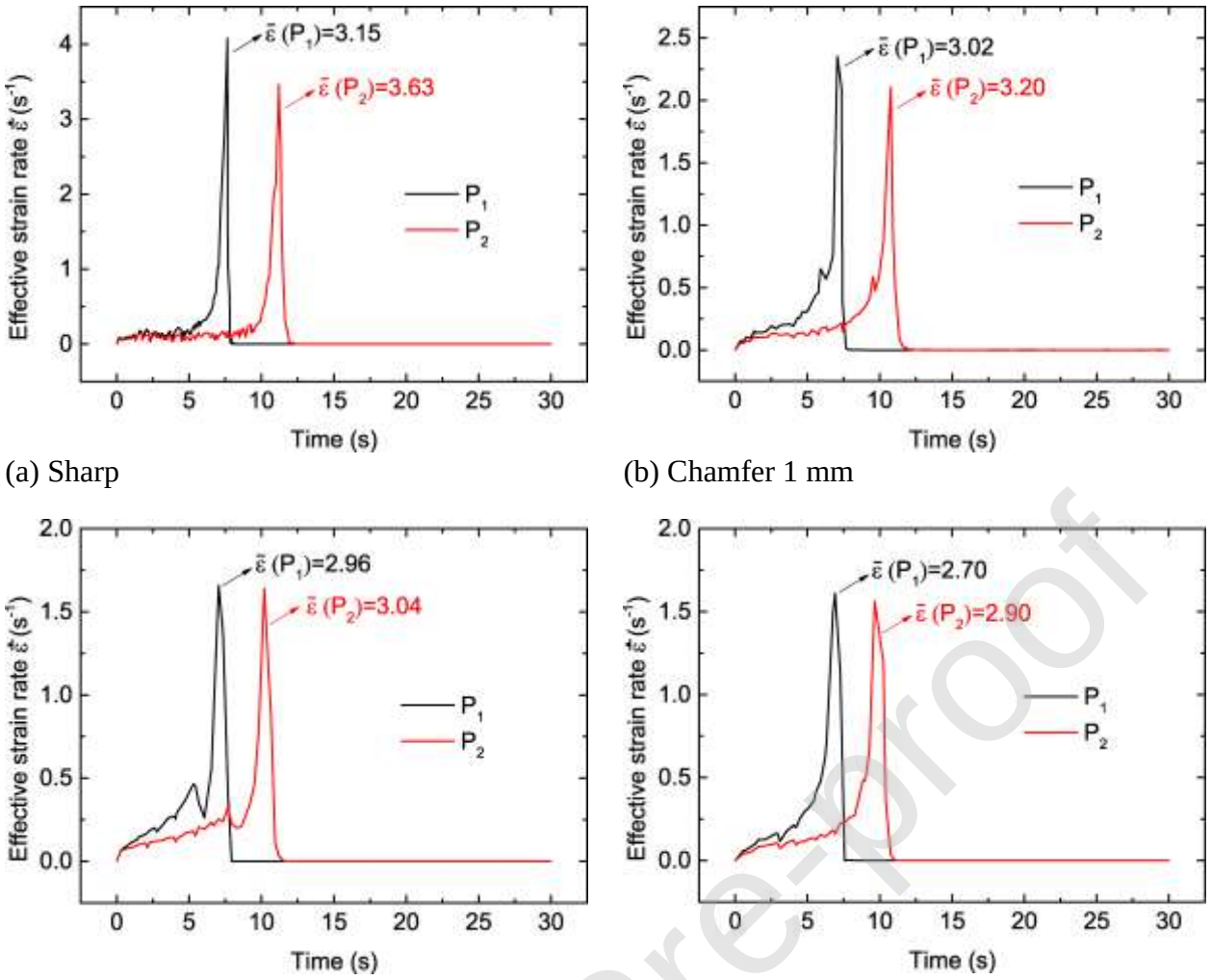

Fig. 15. Evolution of effective strain rate for different die land corner transition geometry: (a) sharp, (b) chamfer 1 mm, (c) chamfer 2 mm, (d) radius 2 mm.

4. Conclusions

Physical experiments and numerical modelling were conducted to investigate the effects of die land length and geometry on curved profiles produced by a novel differential velocity sideways extrusion process. The effects were evaluated in aspects of the curvature of deformed extrudate, strain level and strain homogeneity over the extrudate cross-section. The following conclusions are drawn from the results:

(1) Die land length greatly affects profile curvature due to its influence on exit velocity gradient. Profile curvature decreases as land length increases, and when the ratio l_λ of land length to die orifice diameter exceeds a critical value l_0, a straight profile is extruded. l_0 increases as the extrusion ratio λ increases and extrusion velocity ratio v_2/v_1 decreases, and has an approximate relation of $l_0 = c\lambda^n[1-(v_2/v_1)^m]$, where c = 0.731, n = 0.086, m = 2.50. A die land length ratio l_λ less than l_0 is recommended for an effective and wide control of curvature.

(2) Die land length slightly affects profile overall effective strain level due to its local influence on extrudate surface layer effective strain. As die land length increases, frictional areas between extrudate surface layers and die land (and mandrel for tube extrusion) increase, leading to an increased surface layer effective strain due to zone of shear along the profile surface being generated. Strain homogeneity over the cross-section or wall thickness (for tube extrusion) is decreased as a result of increased surface layer effective strain.

(3) Die land/container with a chamfered or radiused transition corner leads to a greater curvature compared with that resulting from a sharp transition corner. The increase in curvature is attributed to the decrease of effective die land length.

(4) Die land/container transition corner geometry greatly affects the effective strain level and strain homogeneity due to its influence on effective strain rate across the deforming region. A chamfered or radiused transition corner leads to a decreased overall cross-sectional effective strain level and strain homogeneity as a result of dispersed and weaker zones of shear on the intersection planes ('V' shape) of the deforming region. To achieve a relatively large and homogenous effective strain over the cross-section, a sharp die land transition corner is recommended.

CRediT Author Statement

Wenbin Zhou: Conceptualization, Methodology, Validation, Investigation, Formal analysis, Data curation, Visualization, Writing- Original draft preparation. Junquan Yu: Conceptualization, Methodology, Visualization, Investigation, Writing- Reviewing and Editing, Supervision. Jianguo Lin: Conceptualization, Methodology, Writing- Reviewing and Editing, Supervision. Trevor A. Dean: Conceptualization, Writing- Reviewing and Editing

Declaration of interests

The authors declare that they have no known competing financial interests or personal relationships that could have appeared to influence the work reported in this paper.

References

Ajiboye, J.S., Adeyemi, M.B., 2006. Effects of die land on the cold extrusion of lead alloy, J. Mater. Process. Technol. 171, 428-436.

Ajiboye, J.S., Adeyemi, M.B., 2007. Upper bound analysis for extrusion at various die land lengths and shaped profiles, Int. J. Mech. Sci. 49, 335-351.

Altan, T., Boulger, F.W., 1973. Flow stress of metals and its application in metal forming analyses. J. Eng. Ind. 95, 1009-1019.

Basavaraj, V.P., Chakkingal, U., Kumar, T.S.P., 2009. Study of channel angle influence on material flow and strain inhomogeneity in equal channel angular pressing using 3D finite element simulation. J. Mater. Process. Technol. 209, 89-95.

Bay, N., Wanheim, T., Arentoft, M., Andersen, C.B., Bennani B., 1995. An appraisal of numerical and physical modelling for prediction of metal forming processes. Proceedings of the Fourth International Conference on Computational Plasticity-Fundamentals and Applications, Barcelona, Spain, pp. 1343-1354

Castle, A., Flory, R., Gagg, J., 1988. Die design and construction in Europe. Proceedings of the Fourth International Aluminium Extrusion Technology Seminar, Chicago, Washington, pp. 25-34.

Chatti, S., Hermes, M., Kleiner, M., 2007. Three-dimensional bending of profiles by stress superposition. In: Banabic, D. (Ed.), Advanced Methods in Material Forming. Springer Verlag, Berlin, pp. 101-118.

Chen, H., Zhao, G., Zhang, C., Guan, Y., Liu, H., Kou, F, 2011. Numerical simulation of extrusion process and die structure optimization for a complex aluminum multicavity wallboard of high-speed train. Mater. Manuf. Process. 26, 1530-1538.

Cruz, P.J.S., 2013. Structures and Architecture: New concepts, Applications and Challenges, first ed. CRC Press, London.

El Mehtedi, M., Spigarelli, S., Gabrielli, F., Donati, L., 2015. Comparison study of constitutive models in predicting the hot deformation behavior of AA6060 and AA6063 Aluminium alloys. Mater. Today Proc. 2, 4732-4739.

Ghassemali, E., Tan, M.J., Jarfors, A.E.W., Lim, S.C.V., 2013. Progressive microforming process: towards the mass production of micro-parts using sheet metal. Int. J. Adv. Manuf. Technol. 66, 611-621.

Hao, N., Li, K., 2000. Numerical design of the die land for shape extrusion. J. Mater. Process. Technol. 101, 81-84.

Hermes, M., Staupendahl, D., Kleiner, M., 2015. Torque superposed spatial bending. In: Tekkaya, A.E., Homberg, W., Brosius, A. (Eds.), 60 Excellent Inventions in Metal Forming. Springer Verlag, Berlin, pp. 381-385.

Jiang, Z.Y., Liu, X.L., Liu, X.H., Wang, G.D., 2000. Analysis of ribbed-strip rolling by rigid-viscoplastic FEM. Int. J. Mech. Sci. 42, 693-703.

Keife, H., 1993. Extrusion through two dies openings: a 2D upper-bound analysis checked by plasticine experiments. J. Mater. Process. Technol. 37, 189-202.

Lee, G.A., Im, Y.T., 2002. Analysis and die design of flat-die hot extrusion process 2. Numerical design of bearing lengths. Int. J. Mech. Sci. 44, 935-946.

Li, H., Li, S., Zhang, D., 2010. On the selection of outlet channel length and billet length in equal channel angular extrusion. Comput. Mater. Sci. 49, 293-298.

Li, S., Bourke, M.A.M., Beyerlein, I.J., Alexander, D.J., Clausen, B., 2004. Finite element analysis of the plastic deformation zone and working load in equal channel angular extrusion. Mater. Sci. Eng. A 382, 217-236.

Lin, C., Ransing, R.S., 2009. An innovative extrusion die layout design approach for single-hole dies. J. Mater. Process. Technol. 209, 3416-3425.

Meybodi, A. K., Assempour, A., Farahani, S., 2012. A general methodology for bearing design in non-symmetric T-shaped sections in extrusion process. J. Mater. Process. Technol. 212, 249-261.

Müller, K.B., 2006. Bending of extruded profiles during extrusion process. Int. J. Mach. Tool. Manuf. 46, 1238-1242.

Shiraishi, M., Nikawa, M., Goto, Y., 2003. An investigation of the curvature of bars and tubes extruded through inclined dies. Int. J. Mach. Tool. Manuf. 43, 1571-1578.

Takahashi, Y., Kihara, S., Yamaji, K., Shiraishi, M., 2015. Effects of die dimensions for curvature extrusion of curved rectangular bars. Mater. Trans. 56, 844-849.

Tekkaya, A.E., Chatti, S., 2014. Bending (Tubes, Profiles). In: Laperrière, L., Reinhart, G. (Eds.), CIRP Encyclopedia of Production Engineering. Springer Verlag, Berlin, pp. 92-101.

Ulysse, P., 1999. Optimal extrusion die design to achieve flow balance. Int. J. Mach. Tool. Manuf. 39, 1047-1064.

Ulysse, P., 2002. Extrusion die design for flow balance using FE and optimization methods. Int. J. Mech. Sci. 44, 319-341.

Viswanath Ammu, V.N.S.U., Mahendiran, P., Agnihotri, A., Ambade, S., Dungore, P.R, 2018. A simplified approach for generation of bearing curve by velocity distribution and press validation for aluminum extruded profile. Int. J. Adv. Manuf. Technol. 98, 1733-1744.

Vollertsen, F., Sprenger, A., Kraus, J., Arnet, H., 1999. Extrusion, channel, and profile bending: a review. J. Mater. Process. Technol. 87, 1-27.

Xiang, S.W., Wang, G.D., Zhang, Q., 1993. A new model for deformation resistance. J. Iron Steel 28, 21-26.

Yang, H., Li, H., Zhang, Z., Zhan, M., Liu, J., Li, G., 2012. Advances and trends on tube bending forming technologies. Chinese J. Aeronaut. 25, 1-12.

Zhang, S., Extrusion process and die design, Chemical Industry Press, China, 2009, pp.103.

Zhou, W., Lin, J., Dean, T.A., Wang, L., 2018a. Feasibility studies of a novel extrusion process for curved profiles: Experimentation and modelling. Int. J. Mach. Tool. Manuf. 126, 27-43.

Zhou, W., Lin, J., Dean, T.A., Wang, L., 2018b. Analysis and modelling of a novel process for extruding curved metal alloy profiles. Int. J. Mech. Sci. 138, 524-536.

Zhou, W., Yu, J., Lin, J., Dean, T.A., 2019. Manufacturing a curved profile with fine grains and high strength by differential velocity sideways extrusion. Int. J. Mach. Tool. Manuf. 140, 77-88.